



HAL
open science

Closing the hydrogen cycle with the couple sodium borohydride-methanol, via the formation of sodium tetramethoxyborate and sodium metaborate

Kübra Aydın, Büşra Kulakli, Bilge Coşkuner Filiz, Damien Alligier, Umit Demirci, Aysel Kantürk Figen

► **To cite this version:**

Kübra Aydın, Büşra Kulakli, Bilge Coşkuner Filiz, Damien Alligier, Umit Demirci, et al.. Closing the hydrogen cycle with the couple sodium borohydride-methanol, via the formation of sodium tetramethoxyborate and sodium metaborate. *International Journal of Energy Research*, 2020, 44 (14), pp.11405-11416. 10.1002/er.5761 . hal-03544935

HAL Id: hal-03544935

<https://hal.umontpellier.fr/hal-03544935v1>

Submitted on 3 Oct 2022

HAL is a multi-disciplinary open access archive for the deposit and dissemination of scientific research documents, whether they are published or not. The documents may come from teaching and research institutions in France or abroad, or from public or private research centers.

L'archive ouverte pluridisciplinaire **HAL**, est destinée au dépôt et à la diffusion de documents scientifiques de niveau recherche, publiés ou non, émanant des établissements d'enseignement et de recherche français ou étrangers, des laboratoires publics ou privés.

Closing the hydrogen cycle with the couple sodium borohydride-methanol, via the formation of sodium tetramethoxyborate and sodium metaborate

Running title: **Closing the hydrogen cycle with sodium borohydride-methanol**

Kübra Aydın¹, Büşra N. Kulaklı¹, Bilge Coşkuner Filiz², Damien Alligier³, Umit B. Demirci³, Aysel Kantürk Figen^{1*}

¹Department of Chemical Engineering, Yildiz Technical University, İstanbul, Turkey

²Science and Technology Application and Research Center, Yildiz Technical University, İstanbul, Turkey

³Institut Européen des Membranes, IEM – UMR 5635, ENSCM, CNRS, Univ Montpellier, Montpellier, France

* Corresponding author: akanturk@yildiz.edu.tr; ayselkanturk@gmail.com; +90 212 383 47 28

Abstract

Methanolysis of sodium borohydride (NaBH_4) is one of the methods efficient enough to release, on demand, the hydrogen stored in the hydride as well as in 4 equivalents of methanol (CH_3OH). It is generally reported that, in methanolysis, sodium tetramethoxyborate ($\text{NaB}(\text{OCH}_3)_4$) forms as single component of the spent fuel. It is however necessary to clearly investigate some critical aspects related to it. We first focused on the methanolysis reaction where NaBH_4 was reacted with 2, 4, 8, 16 or 32 equivalents of CH_3OH . With 2 equivalents of CH_3OH , the conversion of NaBH_4 is not complete. With 4 to 32 equivalents of CH_3OH , NaBH_4 is totally methanolized (conversion of 100%). The best conditions are those involving 4 equivalents of CH_3OH as they offer the highest effective gravimetric hydrogen storage capacity with 4.8 wt%, an attractive H_2 generation rate with $331 \text{ mL}(\text{H}_2) \text{ min}^{-1}$ – a performance achieved without any catalyst –, and the formation of $\text{NaB}(\text{OCH}_3)_4$ as single product as identified by XRD, FTIR and NMR. We then focused on the transformation of this product $\text{NaB}(\text{OCH}_3)_4$ into sodium metaborate (NaBO_2), via the formation of sodium tetrahydroxyborate ($\text{NaB}(\text{OH})_4$). $\text{NaB}(\text{OCH}_3)_4$ is easily transformed in water, by hydrolysis, at $80 \text{ }^\circ\text{C}$ and for 90 min, into $\text{NaB}(\text{OH})_4$ and 4 equivalents of CH_3OH . In doing so, the cycle with

32 CH₃OH is closed. Subsequently, NaB(OH)₄ is recovered and converted into NaBO₂ under
33 heating at 500 °C. This reaction liberates 4 equivalents of H₂O, which allows to close the cycle
34 with water. Based on these achievements, we have finally proposed a triangular recycling
35 scheme aiming at closing the cycle with the protic reactants of the aforementioned reactions.
36 This scheme may be used as base for implementing a closed cycle with the couple NaBH₄-
37 CH₃OH.

38

39

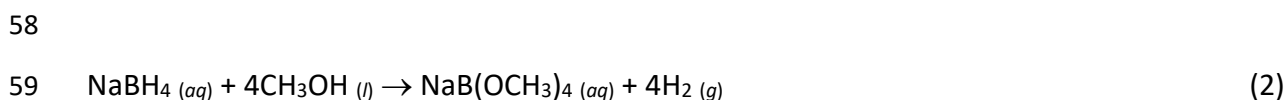
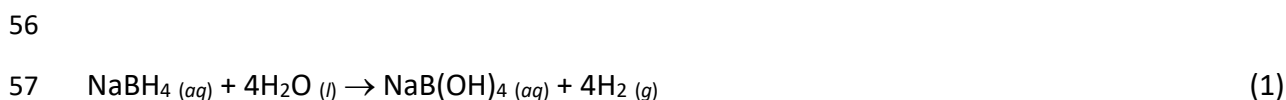
40 **Keywords**

41 Methanolysis; Recycling; Sodium borohydride; Sodium metaborate; Sodium
42 tetramethoxyborate; Spent fuel

43 1. Introduction

44 Hydrogen, owing to its clean nature and high energy density, is clearly one of the most
45 attractive sustainable energy technologies [1]. Hydrogen has grown up very quickly. However,
46 its deployment is confronted with a number of issues touching the whole chain of the so-called
47 “hydrogen economy”. One of the main roadblocks concerns its storage [2]. Various solutions
48 (physical and chemical) have been explored within the past decades [3,4] and chemical
49 hydrogen storage has shown to face a very positive outlook going forward [5–7].

50
51 As chemical hydrogen storage material, sodium borohydride (NaBH₄) has been widely
52 investigated as it is considered as a reliable candidate for mobile applications [2], especially
53 because it carries 10.8 wt% of (atomic) hydrogen (in hydridic form) and is able to readily
54 release (molecular) hydrogen by reaction with water (by hydrolysis [8]) or methanol (by
55 methanolysis [9]) at ambient conditions:



60
61 The reaction, e.g. the hydrolysis one, is spontaneous ($\Delta H = -217 \text{ kJ mol}^{-1}$ at 25 °C) [10] and
62 the solution is generally stabilized by increasing the pH beyond 11 (alkaline conditions) [11].
63 The use of a heterogeneous (metallic) catalyst is required to catalyze the release of hydrogen
64 by hydrolysis [12]. The research field dedicated to NaBH₄ has mainly focused on finding the
65 best catalyst whereas other crucial aspects (by-products, scaling up, among others) have been
66 clearly under-investigated [13].

67
68 One of the main challenges with NaBH₄ is related to the by-product, i.e. sodium
69 tetrahydroxyborate (NaB(OH)₄) in hydrolysis or sodium tetramethoxyborate (NaB(OCH₃)₄) in
70 methanolysis. Recycling it to regenerate NaBH₄ is of importance for closing the hydrogen cycle
71 and for the implementation of the technology. In the field of hydrolysis, a number of studies
72 have focused on identification of the hydrolytic (intermediate and final) by-products [14–16]
73 as well as on regeneration options [17–20], and it may be concluded that the challenge is

74 enormous. Using methanol for dehydrogenating NaBH_4 has advantages over the use of water.
75 One of them is related to the nature of the by-product. In methanolysis (Eq. 2), $\text{NaB}(\text{OCH}_3)_4$
76 forms [21]. Unlike $\text{NaB}(\text{OH})_4$ [22], $\text{NaB}(\text{OCH}_3)_4$ does not have the propensity to readily
77 polymerize into polyborates [23,24], avoiding then their precipitation that are known to cause
78 blocking of pipes and catalyst poisoning [25]. Another attractive feature with $\text{NaB}(\text{OCH}_3)_4$ is
79 that it is one of the intermediate products of the $\text{NaB}(\text{OH})_4$ regeneration process developed
80 by Kemmitt et al. [26]. According to this process, $\text{NaB}(\text{OH})_4$ is first dehydrated into NaBO_2 ,
81 then NaBO_2 is reacted with methanol to form $\text{NaB}(\text{OCH}_3)_4$, and finally $\text{NaB}(\text{OCH}_3)_4$ is reduced
82 into NaBH_4 in the presence of sodium alanate NaAlH_4 in refluxing diglyme. Yet, in
83 methanolysis, $\text{NaB}(\text{OCH}_3)_4$ forms directly (Eq. 2), which then allows getting a cheaper process
84 (free of the two steps of dehydration and methoxylation). To our knowledge, the open
85 literature dedicated to methanolysis of NaBH_4 mainly deals with reaction parameters [27–30],
86 catalysts [27,31–33], and kinetics [23,29,30]. The catalysis topic has been disproportionately
87 investigated with a large number of possible catalysts reported so far [34]. Examples of recent
88 catalysts are as follows: supported cobalt [35–37] and nickel [38] and bimetallics [39,40], TiO_2
89 [41], metallurgic sludge [42], polymer-based systems (e.g. microgels) [43–46], treated
90 microalgae [47,48] and other natural materials like spent coffee [49,50]. With respect to the
91 by-products like $\text{NaB}(\text{OCH}_3)_4$, very few reports focused on their identification and their solid-
92 state structure. Fernandes et al., who primarily investigated the effect of methanol on the
93 kinetics of hydrolysis of NaBH_4 for methanol-water mixtures, showed that $\text{NaB}(\text{OCH}_3)_4$ is only
94 obtained in the absence of water [21]. Huynh et al. isolated and characterized a solid-state
95 methanolysis by-product [51]. By XRD analyses, a derivative of $\text{NaB}(\text{OCH}_3)_4$ was found; the
96 following structure was suggested: $[\text{Na}_2(\text{B}(\text{OCH}_3)_4)_2(\text{CH}_3\text{OH})_2]_4$. Its stability in water was
97 scrutinized; it was observed that hydrolysis takes place resulting in the formation of a hydrated
98 sodium tetraborate salt with the structure $\text{Na}_2[\text{B}_4\text{O}_5(\text{OH})_4] \cdot 8/3\text{H}_2\text{O}$. In this way, methanol
99 (CH_3OH) was recovered.

100

101 In such a context, our efforts have focused on methanolysis of NaBH_4 , specifically on the by-
102 products stemming from this reaction. For a technology that has commercial objectives,
103 implying then large volumes of spent fuel, it is necessary to better understand the by-products
104 as well as to think about economically viable recycling processes. We performed a systematic
105 work on spent fuel stemming from the methanolysis of NaBH_4 . The reaction was performed

106 at the scale of few grams, unlike what is generally reported in the literature, in order to be
107 closer to the technological application. In addition, the reaction was proceeded at different
108 $\text{NaBH}_4/\text{CH}_3\text{OH}$ ratios to check the nature of the spent fuel depending on the amount of CH_3OH
109 and to find the suitable conditions for implementation. Our results have shown the formation
110 of $\text{NaB}(\text{OCH}_3)_4$ only for the ratio 4, which corresponds to the stoichiometric conditions and is
111 the optimal one for a conversion of 100% of NaBH_4 with attractive H_2 generation rates (331
112 $\text{mL}(\text{H}_2) \text{ min}^{-1}$). Otherwise, the methanolysis products obtained for the other ratios, namely 2,
113 8, 16 and 32, were recovered to be analyzed and identified. In a second part of the work, we
114 analyzed the hydrolytic evolution of $\text{NaB}(\text{OCH}_3)_4$ at ambient conditions. It was found to evolve
115 into 4 equivalents of CH_3OH , for which the close is thus closed, and into $\text{NaB}(\text{OH})_4$. The latter
116 product was separated and used to highlight the experimental conditions of its transformation
117 into NaBO_2 . In that respect, the appropriate conditions to transform $\text{NaB}(\text{OCH}_3)_4$ into NaBO_2
118 while recovering CH_3OH have been defined and are discussed in the form of a triangle
119 recycling scheme. This is reported herein.

120

121

122 **2. Experimental procedure**

123 Sodium borohydride (NaBH_4 ; $\geq 98\%$ purity Merck) and anhydrous methanol (CH_3OH ; $\geq 99.9\%$
124 Sigma Aldrich) were used as received. They were stored under inert atmosphere.

125

126 Methanolysis by-products were prepared as follows. NaBH_4 (3 g) was transferred in a three-
127 neck flask (100 mL). Hydrogen evolution (Eq. 2) was started by adding a volume of methanol.
128 The amount of the alcohol was varied such as $x = 2, 4, 8, 16, 32$, where x is the mole number
129 of CH_3OH per mole of NaBH_4 . In other words, the reaction was stoichiometric for $x = 4$ (Eq. 2);
130 we performed one experiment at sub-stoichiometry ($x = 2$), and three other ones at over-
131 stoichiometry ($x = 8, 16, 32$). The reaction temperature was set at 20 ± 2 °C. The three-neck
132 flask was connected to an inverted burette (to measure the volume of the evolving H_2), via a
133 cold trap used to condensate any vapor.

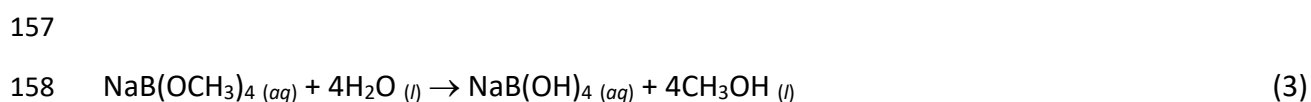
134

135 After the H_2 evolution experiment, the methanolysis spent fuel was recovered. A white solid
136 was obtained for $x = 2, 4$ and 8. For $x = 16$, a white viscous liquid was found to form, and the

137 excess of CH₃OH was removed as follows. The liquid was held at room temperature (under a
138 hood) for 72 h, leading to the formation of white solid powder. For $x = 32$, a colorless liquid
139 was obtained. After extraction of CH₃OH in excess in a similar way, a white solid powder was
140 recovered. The powders were put under vacuum at 40 °C before they were stored in a
141 desiccator. Their morphology was scrutinized by scanning electron microscope (SEM, Zeiss
142 EVO® LS 10).

143
144 The crystal structure of the white solid powders was analyzed by powder X-ray diffraction
145 (XRD; Philips Panalytical X'Pert-Pro, CuK α). Pattern matching was performed using the
146 database available proposed by the PANalytical X'Pert HighScore Plus (PDF-4 2018 RDB)
147 software. The molecular structure was investigated by Fourier transform infrared
148 spectroscopy (FTIR, ATR equipped Perkin Elmer Spectrum One, 4 cm⁻¹). The samples were
149 analyzed by ¹¹B nuclear magnetic resonance (NMR) spectroscopy (Bruker AVANCE-300; probe
150 head BBO10, 96.29 MHz, D₂O or CD₃CN in a capillary tube). Anhydrous N,N-
151 dimethylformamide (HCON(CH₃)₂, Merck) was used to dissolve the solids. Some of the samples
152 were further analyzed by Raman spectroscopy (Horiba Jobin Yvon LabRAM 1B; laser Ar/Kr 100
153 mW 647.1 nm).

154
155 Solid NaB(OCH₃)₄ (recovered for the experiment such as $x = 4$) were then put in water to
156 investigate their possible evolution into e.g. NaB(OH)₄ by hydrolysis:



160 Typically, NaB(OCH₃)₄ (2.46 g) and H₂O (1.25 g) were loaded in a glass batch reactor. The
161 reaction mixture was heated at 80 ± 2 °C, under stirring (500 rpm), and for 90 min. Upon
162 hydrolysis, the slurry was isolated and dried at 60 °C under vacuum atmosphere for 4 h. The
163 as-obtained white solid was analyzed by XRD. Its thermal stability was analyzed by
164 thermogravimetric (TG) analysis and differential thermal (DT) analysis (SII Nanotechnology –
165 SII6000 Exstar TG/DTA 6300; aluminum crucible; temperature range of 50-700°C; heating rate
166 of 10°C min⁻¹) under either oxidative (O₂) or inert (N₂) atmosphere. These TG and DT analyses
167 allowed us choosing the temperatures 300 and 500 °C for calcination of the hydrolysis white

168 solids; alumina high temperature crucibles were used. The as-calcined solids were analyzed
169 by XRD. The formation of NaBO₂ was actually targeted:

170



172

173 Based on Eq. 3, CH₃OH was predicted to form. It was identified by analyzing the slurry using
174 gas chromatography (Perkin Elmer Clarus 580 GC apparatus with split injector and FID
175 detector; 30 m column ID BPX5 with i.d. and film thickness of 0.25 mm and 0.25 μm
176 respectively). The oven temperature program was as follows: initial temperature of 40 °C;
177 heating rate of 15 °C min⁻¹ until 70°C; 3 min at 70 °C; heating rate of 45 °C min⁻¹ until 250 °C;
178 5 min at 250 °C. The injector and detector temperatures were, respectively, 100 and 300 °C.
179 The flow rate of the carrier gas (H₂) was set at 0.5 mL min⁻¹.

180

181 **3. Result and Discussion**

182 **3.1. Towards sodium tetramethoxyborate NaB(OCH₃)₄**

183 At sub-stoichiometric and stoichiometric conditions, i.e. for $x = 2$ and $x = 4$ (Eq. 2), a solid
184 formed by methanolysis of NaBH₄. In the former case, the presence of some unreacted NaBH₄
185 is likely. A repeated experiment where the volume of H₂ was collected showed a partial
186 conversion of NaBH₄, calculated to be as low as about 40% (Figure S1). This is also consistent
187 with the NMR, XRD and FTIR results reported hereafter. In the case of $x = 4$, all of the NaBH₄
188 are ideally supposed to react with 4 equiv CH₃OH to form NaB(OCH₃)₄. This was verified by
189 measuring the volume of the generated H₂ (Figure S1); the H₂ generation rate was calculated
190 (for a conversion ≤ 50%) to be 331 mL(H₂) min⁻¹. A solid was also recovered upon the
191 completion of the reaction involving $x = 8$. The three solids were observed by SEM (Figures S2
192 to S4). They consist of an irregularly-shaped matrix. The surface of the solids obtained for $x =$
193 2 is rougher, likely because of the presence of some unreacted NaBH₄. The surface of the solids
194 obtained for $x = 4$ and $x = 8$ are smoother and comparable, and they may indicate similar
195 products. A white viscous liquid was obtained for $x = 16$, and for the higher ratio, $x = 32$, a
196 colorless liquid was recovered. Actually, at over-stoichiometric conditions, the excess of
197 methanol, that is, the fraction that did not react with NaBH₄, acts as solvent. This excess of
198 methanol was then extracted and white solids were recovered. By SEM (Figures S5 and S6),

199 smaller structures (about 400-600 nm) were observed. They are irregularly-shaped and
200 agglomerated. The smaller size may be a result of the solvent extraction and the related
201 crystallization of the methanolysis product.

202
203 The methanolysis solid by-products were first considered for analysis by ^{11}B NMR
204 spectroscopy. D_2O as deuterated solvent was found to be inappropriate because of e.g.
205 bubbling of the solid obtained for $x = 2$. Note that this confirmed the presence of some
206 unreacted NaBH_4 (quintet at -39.2 ppm) upon hydrolysis in sub-stoichiometric conditions.
207 N,N -Dimethylformamide is a good solvent for NaBH_4 , and the borates are also slightly soluble
208 in it. It was therefore used to dissolve the methanolysis solid by-products. The ^{11}B NMR
209 analyses were performed using CD_3CN as deuterated solvent (Figure 1). The presence of some
210 unreacted NaBH_4 for the reaction at $x = 2$ (i.e. sub-stoichiometry) is confirmed. Borates ($\delta = 3$
211 ppm) formed when methanolysis was performed in stoichiometric and over-stoichiometric
212 conditions (total conversion of NaBH_4). According to Huynh et al. [51], the signal may be
213 ascribed to methanolated methoxyborate like $[\text{Na}_2(\text{B}(\text{OCH}_3)_4)_2(\text{CH}_3\text{OH})_2]_4$.

214
215 The solids were analyzed by XRD (Figure 2). The presence of unreacted NaBH_4 (ref. 00-009-
216 0386) for the reaction performed at $x = 2$ is confirmed. No trace of a crystalline phase of
217 $\text{NaB}(\text{OCH}_3)_4$ was detected, suggesting the formation of an amorphous by-product. There are
218 few peaks, of very low intensity, that have not been identified and indexed. Pattern matching
219 has not given any relevant result. They are likely to belong to one or more unidentified
220 intermediate species or to an unidentified product; compounds with one to four B–O bonds
221 (for example $\text{NaBH}_3(\text{OCH}_3)$ and $\text{NaBH}_2(\text{OCH}_3)_2$), including oligomeric borates made of 2 to 5
222 boron atoms, are possible species. The pattern of the by-product obtained at $x = 4$ well
223 matches that of the referenced structure (ref. 00-012-0863) belonging to $\text{NaB}(\text{OCH}_3)_4$. This is
224 in agreement with the results reported by Fernandes et al. [21]. The XRD patterns of the other
225 by-products (i.e. obtained at $x = 8, 16$ and 32) are different. There are similar to the pattern
226 reported by Huynh et al. [51] found for $[\text{Na}_2(\text{B}(\text{OCH}_3)_4)_2(\text{CH}_3\text{OH})_2]_4$ (tetragonal, s.g. I_4),
227 synthesized by reacting NaBH_4 in an excess of methanol (anhydrous). To sum up our
228 observations, a minimum of 4 equiv CH_3OH is required for methanolysis completion and the
229 reaction results in the formation of $\text{NaB}(\text{OCH}_3)_4$. In an excess of CH_3OH , the by-product is a
230 complex of both $[\text{B}(\text{OCH}_3)_4]^-$ and CH_3OH , like the species $[\text{Na}_2(\text{B}(\text{OCH}_3)_4)_2(\text{CH}_3\text{OH})_2]_4$.

231

232 The solids were analyzed by FTIR (Figure 3). The observed bands have been indexed with
233 database available in the literature [52–54]. The spectrum of the solid obtained at $x = 2$ shows
234 well-defined sharp bands at e.g. 2500-2100 cm^{-1} (B–H stretching), ascribed to unreacted
235 NaBH_4 [55]. There are also bands at wavenumbers typical of O–H stretching (3600-3000 cm^{-1})
236 and B–O stretching (1000-750 cm^{-1}) modes, indicating some conversion of NaBH_4 into a
237 borate intermediate (amorphous to X-ray). The spectrum of the solid obtained at $x = 4$ is
238 comparable to the fingerprint of $\text{NaB}(\text{OCH}_3)_4$ [56]. All of the bands can be ascribed to B–O
239 stretching/deformation, C–O stretching and C–H stretching/deformation modes. The spectra
240 of the solids obtained at $x = 8, 16$ and 32 (Figures 3, and S7 to S9) look like that of a
241 methoxyborate by-product like $\text{NaB}(\text{OCH}_3)_4$. The O–H deformation mode at around 1600 cm^{-1}
242 (as well as the bands due to O–H stretching) indicates the presence of CH_3OH [51], in
243 agreement with the conclusions made from the analysis of the XRD patterns.

244

245 The sample obtained at $x = 4$, i.e. $\text{NaB}(\text{OCH}_3)_4$, was selected for further analyses. Its thermal
246 stability was analyzed under oxidative and inert atmospheres (Figure S10). A comparable
247 behavior was found. The sample decomposes starting from 30 °C. It undergoes four successive
248 weight losses up to 700 °C, with a main one between 60 and 300 °C. The total weight loss is
249 slightly higher than 45 wt%. In other words, $\text{NaB}(\text{OCH}_3)_4$ is not thermally stable.

250

251 **3.2. Towards sodium metaborate NaBO_2**

252 $\text{NaB}(\text{OCH}_3)_4$ (i.e. the solid obtained at $x = 4$) readily reacts with water. Total conversion was
253 found to occur for a $\text{H}_2\text{O}/\text{NaB}(\text{OCH}_3)_4$ molar ratio $n \geq 4$. The formation of CH_3OH was verified
254 by GC–FID (Figure S11). The hydrolytic boron product was heated at 60°C, under vacuum, to
255 remove water. A white solid was recovered.

256

257 The hydrolysis solid was analyzed by XRD (Figure 4). Monoclinic $\text{NaB}(\text{OH})_4$ (ref. 04-011-2875)
258 was found to be the main crystallographic phase. The presence of another hydrated borate
259 (e.g. $\text{Na}_2\text{B}_4\text{O}_7 \cdot 5\text{H}_2\text{O}$, ref. 00-007-0277) is likely. The FTIR spectrum (Figure 5) is consistent with
260 the formation of such hydrated borates [57–59]. The ^{11}B NMR spectrum (Figure 6) of the solid
261 dissolved in deuterated water shows two signals at positive chemical shifts suggesting two

262 borate species [60], which might be due to equilibrium between the BO_3 (due to e.g. H_3BO_3)
263 and BO_4 environments (i.e. $B(OH)_4^-$) [61].

264
265 The hydrolysis solid was heated, up to 300°C. The XRD pattern (Figure 4) indicates a lightly
266 crystalline solid. The few peaks of small intensity were found to indicate the formation of
267 $NaBO_2$ (ref. 00-037-0115). However, the presence of crystalline $Na_2B_4O_{10}$ (ref. 00-022-1347)
268 cannot be discarded as suggested by the pattern matching. The FTIR spectrum (Figure 5)
269 shows an evolution towards dehydration, which is featured by O–H bands with decreased
270 intensity. The ^{11}B NMR spectrum (Figure 6) is comparable to that of the sample heated at 60
271 °C.

272
273 A last heat-treatment was performed at 500°C. Only the rhombohedral $NaBO_2$ phase (ref. 01-
274 076-0750) was identified (Figure 4), consistently with ref. [62]. $NaB(OH)_4$ is known to lose
275 structural water from about 150 °C [57], resulting in the formation of $NaBO_2$. Temperatures
276 of $NaBO_2$ formation of 300 and 400 °C were reported [57,62]. This is quite consistent with our
277 XRD observations. The FTIR spectrum is also consistent with this observation (Figure 5). The
278 ^{11}B NMR spectrum (Figure 6) of $NaBO_2$ dissolved in deuterated water shows one signal at 4.5
279 ppm, ascribed to a BO_4 environments such as for $B(OD)_4^-$.

280
281 The solids heated at 60, 300 and 500 °C were analyzed by Raman spectroscopy (Figure 7). The
282 first two solids show bands due to symmetric ($700-950\text{ cm}^{-1}$) and asymmetric ($350-1100\text{ cm}^{-1}$)
283 stretching of B–O bonds. The bands at about 750 cm^{-1} may be attributed to $B(OH)_3$ species,
284 and that at 942 cm^{-1} to $B(OH)_4^-$ [63]. The band peaking at 1076 cm^{-1} , which is the only one
285 observed for the sample heated at 500 °C, is assigned to $NaBO_2$. These results confirm the
286 XRD, FTIR, and NMR data discussed above, that is, the complete transformation of $NaB(OCH_3)_4$
287 into $NaBO_2$ via $NaB(OH)_4$.

288
289 **3.3. Towards a neutral cycle with $NaBH_4$**

290 What emerges from the patterns and spectra reported above is that the hydrogen cycle with
291 $NaBH_4$ can be neutral. In other words, the methanolysis by-product could be recycled through
292 a stepwise process to form $NaBH_4$ back. This is illustrated in Figure 8.

293
294 Methanolysis of NaBH_4 is an efficient process for H_2 release, resulting in formation of
295 $\text{NaB}(\text{OCH}_3)_4$ as main by-product when the reaction is realized in stoichiometric conditions (Eq.
296 2). Typically, 1 equiv NaBH_4 reacts with 4 equiv CH_3OH and transforms into 1 equiv $\text{NaB}(\text{OCH}_3)_4$
297 while liberating 4 equiv H_2 . Such a reaction is very interesting for two reasons. First, all of the
298 atoms are effectively used resulting in an “atom economy” in good agreement with one of the
299 green chemistry principles. Second, the aforementioned stoichiometry implies an effective
300 gravimetric hydrogen capacity of 4.8 wt% for the couple $\text{NaBH}_4\text{-CH}_3\text{OH}$, and this is a clearly
301 promising capacity. In addition, the H_2 generation rate was calculated to be $331 \text{ mL}(\text{H}_2) \text{ min}^{-1}$
302 (without catalyst), which is one of the best performance for an uncatalyzed solvolysis reaction
303 involving a hydride and a protonic solvent; some examples are shown in Table 1 [21,22,30,64–
304 74].

305
306 The as-formed $\text{NaB}(\text{OCH}_3)_4$ can be readily hydrolyzed into $\text{NaB}(\text{OH})_4$, and 4 equiv CH_3OH are
307 generated. The cycle is then neutral in CH_3OH . With respect to $\text{NaB}(\text{OH})_4$, it is easily converted,
308 under heating up to $500 \text{ }^\circ\text{C}$ in our conditions, into NaBO_2 while releasing 2 equiv H_2O . The
309 other 2 equiv H_2O are generated during reduction of NaBO_2 into NaBH_4 . Hence, the cycle is
310 neutral in H_2O .

311
312 As mentioned just above, NaBO_2 has to be reduced into NaBH_4 . This may be done by using 4
313 equiv H_2 or a reducing agent carrying H^- such as MgH_2 [18,75,76]. Another original procedure,
314 recently reported [77], could be to make react NaBO_2 with CO_2 in aqueous solution, the as-
315 forming $\text{Na}_2\text{B}_4\text{O}_7 \cdot 10\text{H}_2\text{O}$ and Na_2CO_3 being afterwards ball-milled with Mg under ambient
316 conditions to form NaBH_4 in a yield close to 80 %. In any case, the cycle is then neutral in H_2 .
317 It is worth mentioning that regeneration of NaBH_4 starting from NaBO_2 has been
318 demonstrated, but the processes developed so far need to be further improved to make
319 one/few of them cost-effective [78]. Another challenge, with these processes, will be to
320 develop them while the cycle of each reactant and product is neutral. Otherwise, the scheme
321 of the recycling process could be considered differently for the third part, namely
322 transformation of $\text{NaB}(\text{OH})_4$ into NaBH_4 via NaBO_2 . In the recent years, Ouyang and co-workers
323 reported few regeneration routes using $\text{NaBO}_2 \cdot x\text{H}_2\text{O}$ (with $x = 2$ or 4) as starting borate. Ball-
324 milling $\text{NaBO}_2 \cdot x\text{H}_2\text{O}$ with MgH_2 at room temperature and atmospheric pressure was found to

325 lead to NaBH₄ back with a yield as high as 90% [79]. In another work, Mg was used instead of
326 MgH₂ and NaBH₄ was regenerated with yields of 64-68% [80]. The formation of NaBH₄ was
327 explained by the involvement of reaction intermediates like MgH₂ and NaBH₃(OH).

328

329 **4. Conclusion**

330 In the present work, we have proposed a neutral cycle for the hydrogen storage system based
331 on the couple NaBH₄-4CH₃OH. Upon methanolysis, this couple releases 4 equiv H₂ in such a
332 way that the effective gravimetric hydrogen capacity is as high as 4.8 wt%, which is quite
333 attractive from an implementation point of view. It is worth mentioning the H₂ generation rate
334 that has been achieved without any catalyst, namely, 331 mL(H₂) min⁻¹. The methanolysis by-
335 product is NaB(OCH₃)₄. By using 4 equiv H₂O, NaB(OCH₃)₄ can be readily hydrolyzed to
336 NaB(OH)₄. The process generates 4 equiv CH₃OH, making the cycle neutral in CH₃OH. Then,
337 NaB(OH)₄ can be converted, under heating up to 500 °C, into NaBO₂ which is the most
338 common starting material for regenerating NaBH₄. In a further step, NaBO₂ could be reduced
339 into NaBH₄ while using 4 equiv H₂ or e.g. 4 equiv MgH₂. The cycle would be neutral in H₂. Each
340 of the NaB(OH)₄ heating and NaBO₂ reduction processes generates 2 equiv H₂O, making the
341 cycle neutral in H₂O also. The cycle summarized above is thus also neutral in the B element;
342 indeed the starting NaBH₄ is targeted to be regenerated by recovering all of the formed
343 NaB(OH)₄ via its total conversion into NaB(OH)₄ and then NaBO₂. In that respect, all of the
344 atoms involved in this cycle are used and re-used, resulting in an “atom economy” in good
345 agreement with one of the green chemistry principles. In conclusion, the strategy we propose
346 will help us in building a closed pathway from NaBH₄ to its spent fuel without disturbing the
347 environmental balance.

348

349 **Acknowledgements**

350 This work was supported by TUBITAK (Project no: 218M181) and CAMPUS FRANCE – PHC
351 BOSPHORUS (Project no: 42161TB). UBD and DA thank the Agence Nationale de la Recherche
352 (Project MOBIDIC; ANR-16-CE05-0009).

353

354

355

356 References

- 357 [1] Saeedmanesh A, Mac Kinnon MA, Brouwer J. Hydrogen is essential for sustainability.
358 Curr Opin Electrochem 2018;12:166–81. <https://doi.org/10.1016/j.coelec.2018.11.009>.
- 359 [2] Abe JO, Popoola API, Ajenifuja E, Popoola OM. Hydrogen energy, economy and storage:
360 review and recommendation. Int J Hydrogen Energy 2019;44:15072–86.
361 <https://doi.org/10.1016/j.ijhydene.2019.04.068>.
- 362 [3] Müller K, Arlt W. Status and development in hydrogen transport and storage for energy
363 applications. Energy Technol 2013;1:501–11.
364 <https://doi.org/10.1002/ente.201300055>.
- 365 [4] Abdalla AM, Hossain S, Nisfindy OB, Azad AT, Dawood M, Azad AK. Hydrogen
366 production, storage, transportation and key challenges with applications: a review.
367 Energy Convers Manag 2018;165:602–27.
368 <https://doi.org/10.1016/j.enconman.2018.03.088>.
- 369 [5] Hirscher M, Yartys VA, Baricco M, Bellosta von Colbe J, Blanchard D, Bowman RC, et al.
370 Materials for hydrogen-based energy storage – past, recent progress and future
371 outlook. J Alloys Compd 2020;827:153548.
372 <https://doi.org/10.1016/j.jallcom.2019.153548>.
- 373 [6] Kojima Y. Hydrogen storage materials for hydrogen and energy carriers. Int J Hydrogen
374 Energy 2019;44:18179–92. <https://doi.org/10.1016/j.ijhydene.2019.05.119>.
- 375 [7] Wang K, Pan Z, Yu X. Metal B-N-H hydrogen-storage compound: development and
376 perspectives. J Alloys Compd 2019;794:303–24.
377 <https://doi.org/10.1016/j.jallcom.2019.04.240>.
- 378 [8] Davis RE, Bromels E, Kibby CL. Boron hydrides III. hydrolysis of sodium borohydride in
379 aqueous solution. J Am Chem Soc 1962;84:885–92.
380 <https://doi.org/10.1021/ja00865a001>.
- 381 [9] Davis RE, Gottbrath JA. Boron hydrides V. methanolysis of sodium borohydride. J Am
382 Chem Soc 1962;84:895–8. <https://doi.org/10.1021/ja00865a003>.
- 383 [10] Kojima Y, Suzuki K, Fukumoto K, Sasaki M, Yamamoto T, Kawai Y, et al. Hydrogen
384 generation using sodium borohydride solution and metal catalyst coated on metal
385 oxide. Int J Hydrogen Energy 2002;27:1029–34. [https://doi.org/10.1016/S0360-3199\(02\)00014-9](https://doi.org/10.1016/S0360-3199(02)00014-9).
- 386

- 387 [11] Kim JH, Kim KT, Kang YM, Kim HS, Song MS, Lee YJ, et al. Study on degradation of
388 filamentary Ni catalyst on hydrolysis of sodium borohydride. *J Alloys Compd*
389 2004;379:222–7. <https://doi.org/10.1016/j.jallcom.2004.02.009>.
- 390 [12] Brack P, Dann SE, Wijayantha KGU. Heterogeneous and homogenous catalysts for
391 hydrogen generation by hydrolysis of aqueous sodium borohydride (NaBH₄) solutions.
392 *Energy Sci Eng* 2015;3:174–88. <https://doi.org/10.1002/ese3.67>.
- 393 [13] Lang C, Jia Y, Yao X. Recent advances in liquid-phase chemical hydrogen storage. *Energy*
394 *Storage Mater* 2020;26:290–312. <https://doi.org/10.1016/j.ensm.2020.01.010>.
- 395 [14] Kantürk Figen A, Öztürk A, Pişkin S. Process for the conversion of highly caustic spent
396 sodium borohydride fuel. *Res Chem Intermed* 2012;38:2343–54.
397 <https://doi.org/10.1007/s11164-012-0550-9>.
- 398 [15] Hsueh CL, Liu CH, Chen BH, Chen CY, Kuo YC, Hwang KJ, et al. Regeneration of spent-
399 NaBH₄ back to NaBH₄ by using high-energy ball milling. *Int J Hydrogen Energy*
400 2009;34:1717–25. <https://doi.org/10.1016/j.ijhydene.2008.12.036>.
- 401 [16] Stepanov N, Uvarov V, Popov I, Sasson Y. Study of by-product of NaBH₄ hydrolysis and
402 its behavior at a room temperature. *Int J Hydrogen Energy* 2008;33:7378–84.
403 <https://doi.org/10.1016/j.ijhydene.2008.09.052>.
- 404 [17] Qin C, Ouyang L, Wang H, Liu J, Shao H, Zhu M. Regulation of high-efficient regeneration
405 of sodium borohydride by magnesium-aluminum alloy. *Int J Hydrogen Energy*
406 2019;44:29108–15. <https://doi.org/10.1016/j.ijhydene.2019.05.010>.
- 407 [18] Çakanyıldırım Ç, Gürü M. Processing of NaBH₄ from NaBO₂ with MgH₂ by ball milling
408 and usage as hydrogen carrier. *Renew Energy* 2010;35:1895–9.
409 <https://doi.org/10.1016/j.renene.2010.01.001>.
- 410 [19] Kojima Y, Haga T. Recycling process of sodium metaborate to sodium borohydride. *Int*
411 *J Hydrogen Energy* 2003;28:989–93. [https://doi.org/10.1016/S0360-3199\(02\)00173-8](https://doi.org/10.1016/S0360-3199(02)00173-8).
- 412 [20] Li ZP, Morigazaki N, Liu BH, Suda S. Preparation of sodium borohydride by the reaction
413 of MgH₂ with dehydrated borax through ball milling at room temperature. *J Alloys*
414 *Compd* 2003;349:232–6. [https://doi.org/10.1016/S0925-8388\(02\)00872-1](https://doi.org/10.1016/S0925-8388(02)00872-1).
- 415 [21] Fernandes VR, Pinto AMFR, Rangel CM. Hydrogen production from sodium borohydride
416 in methanol–water mixtures. *Int J Hydrogen Energy* 2010;35:9862–8.
417 <https://doi.org/10.1016/j.ijhydene.2009.11.064>.
- 418 [22] Yu L, Matthews MA. Hydrolysis of sodium borohydride in concentrated aqueous

- 419 solution. Int J Hydrogen Energy 2011;36:7416–22.
420 <https://doi.org/10.1016/j.ijhydene.2011.03.089>.
- 421 [23] Lo CTF, Karan K, Davis BR. Kinetic assessment of catalysts for the methanolysis of
422 sodium borohydride for hydrogen generation. Ind Eng Chem Res 2009;48:5177–84.
423 <https://doi.org/10.1021/ie8009186>.
- 424 [24] Ocon JD, Tuan TN, Yi Y, de Leon RL, Lee JK, Lee J. Ultrafast and stable hydrogen
425 generation from sodium borohydride in methanol and water over Fe–B nanoparticles.
426 J Power Sources 2013;243:444–50. <https://doi.org/10.1016/j.jpowsour.2013.06.019>.
- 427 [25] Lapeña-Rey N, Blanco JA, Ferreyra E, Lemus JL, Pereira S, Serrot E. A fuel cell powered
428 unmanned aerial vehicle for low altitude surveillance missions. Int J Hydrogen Energy
429 2017;42:6926–40. <https://doi.org/10.1016/j.ijhydene.2017.01.137>.
- 430 [26] Kemmitt T, Gainsford GJ. Regeneration of sodium borohydride from sodium
431 metaborate, and isolation of intermediate compounds. Int J Hydrogen Energy
432 2009;34:5726–31. <https://doi.org/10.1016/j.ijhydene.2009.05.108>.
- 433 [27] Xu D, Lai X, Guo W, Zhang X, Wang C, Dai P. Efficient catalytic properties of $\text{SO}_4^{2-}/\text{MxO}_y$
434 (M=Cu, Co, Fe) catalysts for hydrogen generation by methanolysis of sodium
435 borohydride. Int J Hydrogen Energy 2018;43:6594–602.
436 <https://doi.org/10.1016/j.ijhydene.2018.02.074>.
- 437 [28] Su CC, Lu MC, Wang SL, Huang YH. Ruthenium immobilized on Al_2O_3 pellets as a catalyst
438 for hydrogen generation from hydrolysis and methanolysis of sodium borohydride. RSC
439 Adv 2012;2:2073. <https://doi.org/10.1039/c2ra01233b>.
- 440 [29] Lo CTF, Karan K, Davis BR. Kinetic studies of reaction between sodium borohydride and
441 methanol, water, and their mixtures. Ind Eng Chem Res 2007;46:5478–84.
442 <https://doi.org/10.1021/ie0608861>.
- 443 [30] Ramya K, Dhathathreyan KS, Sreenivas J, Kumar S, Narasimhan S. Hydrogen production
444 by alcoholysis of sodium borohydride. Int J Energy Res 2013;37:1889–95.
445 <https://doi.org/10.1002/er.3006>.
- 446 [31] Ali F, Khan SB, Asiri AM. Enhanced H_2 generation from NaBH_4 hydrolysis and
447 methanolysis by cellulose micro-fibrous cottons as metal templated catalyst. Int J
448 Hydrogen Energy 2018;43:6539–50. <https://doi.org/10.1016/j.ijhydene.2018.02.008>.
- 449 [32] Demirci S, Yildiz M, Inger E, Sahiner N. Porous carbon particles as metal-free superior
450 catalyst for hydrogen release from methanolysis of sodium borohydride. Renew Energy

- 451 2020;147:69–76. <https://doi.org/10.1016/j.renene.2019.08.131>.
- 452 [33] Xu D, Zhang Y, Cheng F, Zhao L. Enhanced hydrogen generation by methanolysis of
453 sodium borohydride in the presence of phosphorus modified boehmite. *Fuel*
454 2014;134:257–62. <https://doi.org/10.1016/j.fuel.2014.05.071>.
- 455 [34] Özkar S. Transition metal nanoparticle catalysts in releasing hydrogen from the
456 methanolysis of ammonia borane. *Int J Hydrogen Energy* 2020;45:7881–91.
457 <https://doi.org/10.1016/j.ijhydene.2019.04.125>.
- 458 [35] Xu D, Zhang X, Zhao X, Dai P, Wang C, Gao J, et al. Stability and kinetic studies of MOF-
459 derived carbon-confined ultrafine Co catalyst for sodium borohydride hydrolysis. *Int J*
460 *Energy Res* 2019;43:3702–10. <https://doi.org/10.1002/er.4524>.
- 461 [36] Kaya M, Bekiroğullari M, Saka C. Highly efficient CoB catalyst using a support material
462 based on *Spirulina* microalgal strain treated with $ZnCl_2$ for hydrogen generation via
463 sodium borohydride methanolysis. *Int J Energy Res* 2019;43:4243–52.
464 <https://doi.org/10.1002/er.4548>.
- 465 [37] Bekiroğullari M, Kaya M, Saka C. Highly efficient Co-B catalysts with *Chlorella Vulgaris*
466 microalgal strain modified using hydrochloric acid as a new support material for
467 hydrogen production from methanolysis of sodium borohydride. *Int J Hydrogen Energy*
468 2019;44:7262–75. <https://doi.org/10.1016/j.ijhydene.2019.01.246>.
- 469 [38] Wang F, Luo Y, Wang Y, Zhu H. The preparation and performance of a novel spherical
470 spider web-like structure Ru-Ni/Ni foam catalyst for $NaBH_4$ methanolysis. *Int J*
471 *Hydrogen Energy* 2019;44:13185–94. <https://doi.org/10.1016/j.ijhydene.2019.01.123>.
- 472 [39] Zhang Y, Zou J, Luo Y, Wang F. Study on preparation and performance of Ru-Fe/GO
473 catalyst for sodium borohydride alcoholysis to produce hydrogen. *Fullerenes, Nanotub*
474 *Carbon Nanostructures* 2020:1–8. <https://doi.org/10.1080/1536383X.2020.1760849>.
- 475 [40] Tunç N, Rakap M. Preparation and characterization of Ni-M (M: Ru, Rh, Pd) nanoclusters
476 as efficient catalysts for hydrogen evolution from ammonia borane methanolysis.
477 *Renew Energy* 2020;155:1222–30. <https://doi.org/10.1016/j.renene.2020.04.079>.
- 478 [41] Demirci S, Sunol AK, Sahiner N. Catalytic activity of amine functionalized titanium
479 dioxide nanoparticles in methanolysis of sodium borohydride for hydrogen generation.
480 *Appl Catal B Environ* 2020;261:118242. <https://doi.org/10.1016/j.apcatb.2019.118242>.
- 481 [42] Fangaj E, Ali AA, Güngör F, Bektaş S, Ceyhan AA. The use of metallurgical waste sludge
482 as a catalyst in hydrogen production from sodium borohydride. *Int J Hydrogen Energy*

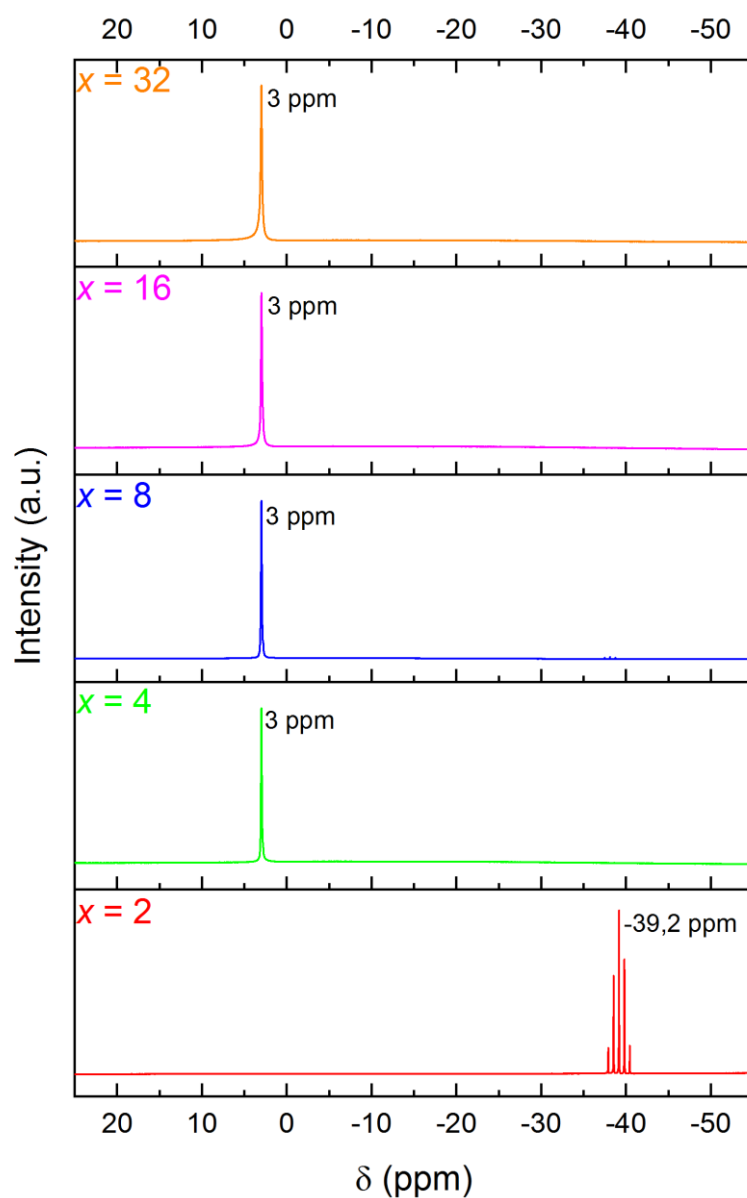
- 483 2020;45:13322–9. <https://doi.org/10.1016/j.ijhydene.2020.03.043>.
- 484 [43] Sahiner N, Demirci S. Very fast H₂ production from the methanolysis of NaBH₄ by metal-
485 free poly(ethylene imine) microgel catalysts. *Int J Energy Res* 2017;41:736–46.
486 <https://doi.org/10.1002/er.3679>.
- 487 [44] Ari B, Ay M, Sunol AK, Sahiner N. Surface-modified carbon black derived from used car
488 tires as alternative, reusable, and regenerable catalysts for H₂ release studies from
489 sodium borohydride methanolysis. *Int J Energy Res* 2019;43:7159–72.
490 <https://doi.org/10.1002/er.4742>.
- 491 [45] Inger E, Sunol AK, Sahiner N. Catalytic activity of metal-free amine-modified dextran
492 microgels in hydrogen release through methanolysis of NaBH₄. *Int J Energy Res* 2020.
493 <https://doi.org/10.1002/er.5395>.
- 494 [46] Khan SB, Ali F, Asiri AM. Metal nanoparticles supported on polyacrylamide water beads
495 as catalyst for efficient generation of H₂ from NaBH₄ methanolysis. *Int J Hydrogen
496 Energy* 2020;45:1532–40. <https://doi.org/10.1016/j.ijhydene.2019.11.042>.
- 497 [47] Saka C, Kaya M, Bekiroğullari M. Spirulina microalgal strain as efficient a metal-free
498 catalyst to generate hydrogen via methanolysis of sodium borohydride. *Int J Energy Res*
499 2020;44:402–10. <https://doi.org/10.1002/er.4936>.
- 500 [48] Kaya M. NiB loaded acetic acid treated microalgae strain (*Spirulina Platensis*) to use as
501 a catalyst for hydrogen generation from sodium borohydride methanolysis. *Energy
502 Sources, Part A Recover Util Environ Eff* 2019;41:2549–60.
503 <https://doi.org/10.1080/15567036.2019.1647312>.
- 504 [49] Kaya M. Production of metal-free catalyst from defatted spent coffee ground for
505 hydrogen generation by sodium borohydride methanolysis. *Int J Hydrogen Energy*
506 2020;45:12731–42. <https://doi.org/10.1016/j.ijhydene.2019.08.013>.
- 507 [50] Kaya M. Evaluating organic waste sources (spent coffee ground) as metal-free catalyst
508 for hydrogen generation by the methanolysis of sodium borohydride. *Int J Hydrogen
509 Energy* 2020;45:12743–54. <https://doi.org/10.1016/j.ijhydene.2019.10.180>.
- 510 [51] Huynh K, Napolitano K, Wang R, Jessop PG, Davis BR. Indirect hydrolysis of sodium
511 borohydride: Isolation and crystallographic characterization of methanolysis and
512 hydrolysis by-products. *Int J Hydrogen Energy* 2013;38:5775–82.
513 <https://doi.org/10.1016/j.ijhydene.2013.03.011>.
- 514 [52] Concha BM, Chatenet M, Coutanceau C, Hahn F. In situ infrared (FTIR) study of the

- 515 borohydride oxidation reaction. *Electrochem Commun* 2009;11:223–6.
516 <https://doi.org/10.1016/j.elecom.2008.11.018>.
- 517 [53] Lixia Z, Tao Y, Jiang W, Shiyang G. FT-IR and Raman spectroscopic study of hydrated
518 rubidium (cesium) borates and alkali double borates. *Russ J Inorg Chem* 2007;52:1786–
519 92. <https://doi.org/10.1134/S0036023607110241>.
- 520 [54] Jun L, Shuping X, Shiyang G. FT-IR and Raman spectroscopic study of hydrated borates.
521 *Spectrochim Acta Part A Mol Biomol Spectrosc* 1995;51:519–32.
522 [https://doi.org/10.1016/0584-8539\(94\)00183-C](https://doi.org/10.1016/0584-8539(94)00183-C).
- 523 [55] Sljukic B, Santos DMF, Sequeira CAC, Banks CE. Analytical monitoring of sodium
524 borohydride. *Anal Methods* 2013;5:829. <https://doi.org/10.1039/c2ay26077h>.
- 525 [56] Xu D, Zhao L, Dai P, Ji S. Hydrogen generation from methanolysis of sodium borohydride
526 over Co/Al₂O₃ catalyst. *J Nat Gas Chem* 2012;21:488–94.
527 [https://doi.org/10.1016/S1003-9953\(11\)60395-2](https://doi.org/10.1016/S1003-9953(11)60395-2).
- 528 [57] Kantürk Figen A, Sari M, Pişkin S. Synthesis, crystal structure and dehydration kinetics
529 of NaB(OH)₄·2H₂O. *Korean J Chem Eng* 2008;25:1331–7.
530 <https://doi.org/10.1007/s11814-008-0218-8>.
- 531 [58] Zhong H, Ouyang LZ, Ye JS, Liu JW, Wang H, Yao XD, et al. An one-step approach towards
532 hydrogen production and storage through regeneration of NaBH₄. *Energy Storage*
533 *Mater* 2017;7:222–8. <https://doi.org/10.1016/j.ensm.2017.03.001>.
- 534 [59] Netskina OV, Komova OV, Simagina VI, Odegova GV, Prosvirin IP, Bulavchenko OA.
535 Aqueous-alkaline NaBH₄ solution: the influence of storage duration of solutions on
536 reduction and activity of cobalt catalysts. *Renew Energy* 2016;99:1073–81.
537 <https://doi.org/10.1016/j.renene.2016.08.005>.
- 538 [60] Chandra M, Xu Q. Dissociation and hydrolysis of ammonia-borane with solid acids and
539 carbon dioxide: an efficient hydrogen generation system. *J Power Sources*
540 2006;159:855–60. <https://doi.org/10.1016/j.jpowsour.2005.12.033>.
- 541 [61] Salentine CG. High-field boron-11 NMR of alkali borates. Aqueous polyborate equilibria.
542 *Inorg Chem* 1983;22:3920–4. <https://doi.org/10.1021/ic00168a019>.
- 543 [62] Kantürk Figen A, Pişkin S. Parametric investigation on anhydrous sodium metaborate
544 (NaBO₂) synthesis from concentrated tincal. *Adv Powder Technol* 2010;21:513–20.
545 <https://doi.org/10.1016/j.apt.2010.01.012>.
- 546 [63] Applegarth L, Pye CC, Cox JS, Tremaine PR. Raman spectroscopic and ab initio

- 547 investigation of aqueous boric acid, borate, and polyborate speciation from 25 to 80 °C.
548 *Ind Eng Chem Res* 2017;56:13983–96. <https://doi.org/10.1021/acs.iecr.7b03316>.
- 549 [64] Weng B, Wu Z, Li Z, Yang H, Leng H. Hydrogen generation from noncatalytic hydrolysis
550 of $\text{LiBH}_4/\text{NH}_3\text{BH}_3$ mixture for fuel cell applications. *Int J Hydrogen Energy*
551 2011;36:10870–6. <https://doi.org/10.1016/j.ijhydene.2011.06.009>.
- 552 [65] Zhang J, Lin F, Yang L, He Z, Huang X, Zhang D, et al. Ultrasmall Ru nanoparticles
553 supported on chitin nanofibers for hydrogen production from NaBH_4 hydrolysis.
554 *Chinese Chem Lett* 2019. <https://doi.org/10.1016/j.ccllet.2019.11.042>.
- 555 [66] Yang L, Huang X, Zhang J, Dong H. Protonated Poly(ethylene imine)-Coated Silica
556 Nanoparticles for Promoting Hydrogen Generation from the Hydrolysis of Sodium
557 Borohydride. *Chempluschem* 2020;85:399–404.
558 <https://doi.org/10.1002/cplu.201900609>.
- 559 [67] Keçeli E, Özkar S. Ruthenium(III) acetylacetonate: A homogeneous catalyst in the
560 hydrolysis of sodium borohydride. *J Mol Catal A Chem* 2008;286:87–91.
561 <https://doi.org/10.1016/j.molcata.2008.02.008>.
- 562 [68] Arzac GM, Fernández A. Hydrogen production through sodium borohydride
563 ethanolysis. *Int J Hydrogen Energy* 2015;40:5326–32.
564 <https://doi.org/10.1016/j.ijhydene.2015.01.115>.
- 565 [69] Saka C, Balbay A. Fast and effective hydrogen production from ethanolysis and
566 hydrolysis reactions of potassium borohydride using phosphoric acid. *Int J Hydrogen*
567 *Energy* 2018;43:19976–83. <https://doi.org/10.1016/j.ijhydene.2018.09.048>.
- 568 [70] Chen J, Fu H, Xiong Y, Xu J, Zheng J, Li X. MgCl_2 promoted hydrolysis of MgH_2
569 nanoparticles for highly efficient H_2 generation. *Nano Energy* 2014;10:337–43.
570 <https://doi.org/10.1016/j.nanoen.2014.10.002>.
- 571 [71] Figen AK, Taşçı K. Hydrolysis characteristics of calcium hydride (CaH_2) powder in the
572 presence of ethylene glycol, methanol, and ethanol for controllable hydrogen
573 production. *Energy Sources, Part A Recover Util Environ Eff* 2016;38:37–42.
574 <https://doi.org/10.1080/15567036.2015.1043473>.
- 575 [72] Ramachandran PV, Gagare PD. Preparation of ammonia borane in high yield and purity,
576 methanolysis, and regeneration. *Inorg Chem* 2007;46:7810–7.
577 <https://doi.org/10.1021/ic700772a>.
- 578 [73] Inoue H, Yamazaki T, Kitamura T, Shimada M, Chiku M, Higuchi E. Electrochemical

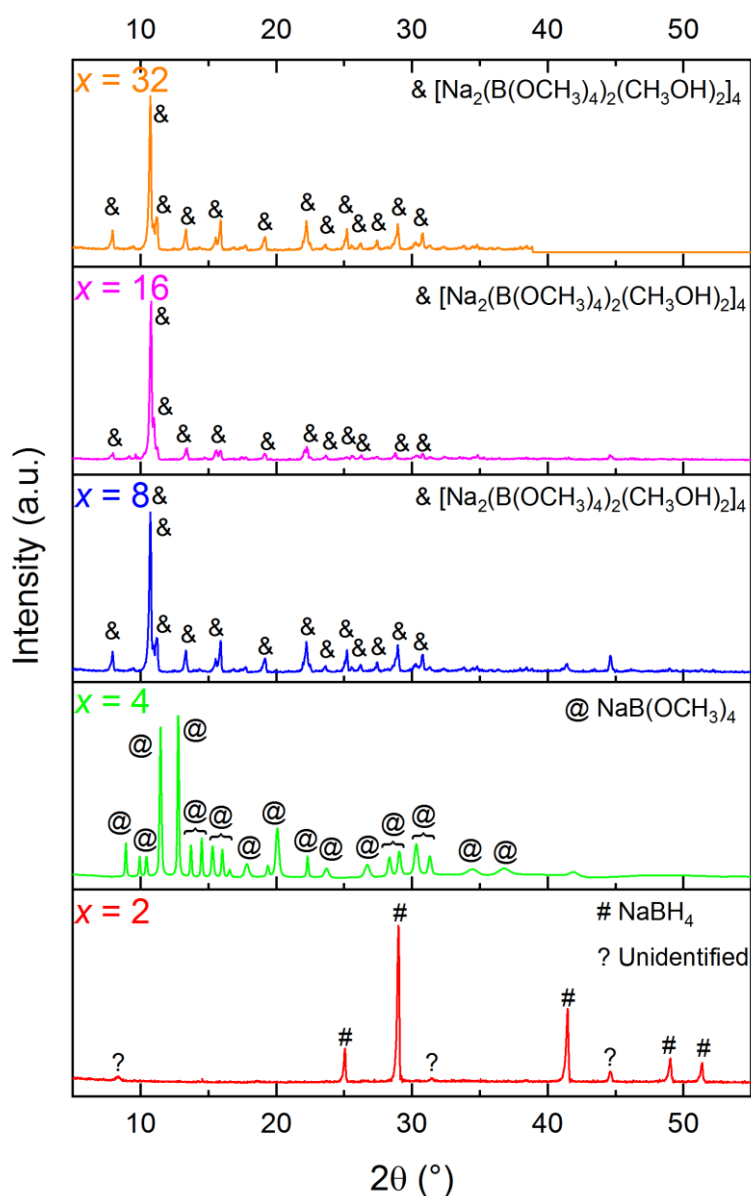
- 579 hydrogen production system from ammonia borane in methanol solution. *Electrochim*
580 *Acta* 2012;82:392–6. <https://doi.org/10.1016/j.electacta.2012.05.091>.
- 581 [74] Weng B, Wu Z, Li Z, Yang H. Hydrogen generation from hydrolysis of MNH_2BH_3 and
582 $\text{NH}_3\text{BH}_3/\text{MH}$ ($\text{M}=\text{Li}, \text{Na}$) for fuel cells based unmanned submarine vehicles application.
583 *Energy* 2012;38:205–11. <https://doi.org/10.1016/j.energy.2011.12.012>.
- 584 [75] Hsueh C-L, Liu C-H, Chen B-H, Chen C-Y, Kuo Y-C, Hwang K-J, et al. Regeneration of
585 spent- NaBH_4 back to NaBH_4 by using high-energy ball milling. *Int J Hydrogen Energy*
586 2009;34:1717–25. <https://doi.org/10.1016/j.ijhydene.2008.12.036>.
- 587 [76] Lang C, Jia Y, Liu J, Wang H, Ouyang L, Zhu M, et al. NaBH_4 regeneration from NaBO_2 by
588 high-energy ball milling and its plausible mechanism. *Int J Hydrogen Energy*
589 2017;42:13127–35. <https://doi.org/10.1016/j.ijhydene.2017.04.014>.
- 590 [77] Zhu Y, Ouyang L, Zhong H, Liu J, Wang H, Shao H, et al. Closing the loop for hydrogen
591 storage: facile regeneration of NaBH_4 from its hydrolytic product. *Angew Chemie Int Ed*
592 2020;59:8623–9. <https://doi.org/10.1002/anie.201915988>.
- 593 [78] Ouyang L, Zhong H, Li H-W, Zhu M. A recycling hydrogen supply system of NaBH_4 based
594 on a facile regeneration process: A review. *Inorganics* 2018;6:10.
595 <https://doi.org/10.3390/inorganics6010010>.
- 596 [79] Chen W, Ouyang LZ, Liu JW, Yao XD, Wang H, Liu ZW, et al. Hydrolysis and regeneration
597 of sodium borohydride (NaBH_4) – A combination of hydrogen production and storage.
598 *J Power Sources* 2017;359:400–7. <https://doi.org/10.1016/j.jpowsour.2017.05.075>.
- 599 [80] Ouyang L, Chen W, Liu J, Felderhoff M, Wang H, Zhu M. Enhancing the regeneration
600 process of consumed NaBH_4 for hydrogen storage. *Adv Energy Mater* 2017;7:1700299.
601 <https://doi.org/10.1002/aenm.201700299>.

602
603
604
605
606
607
608
609
610



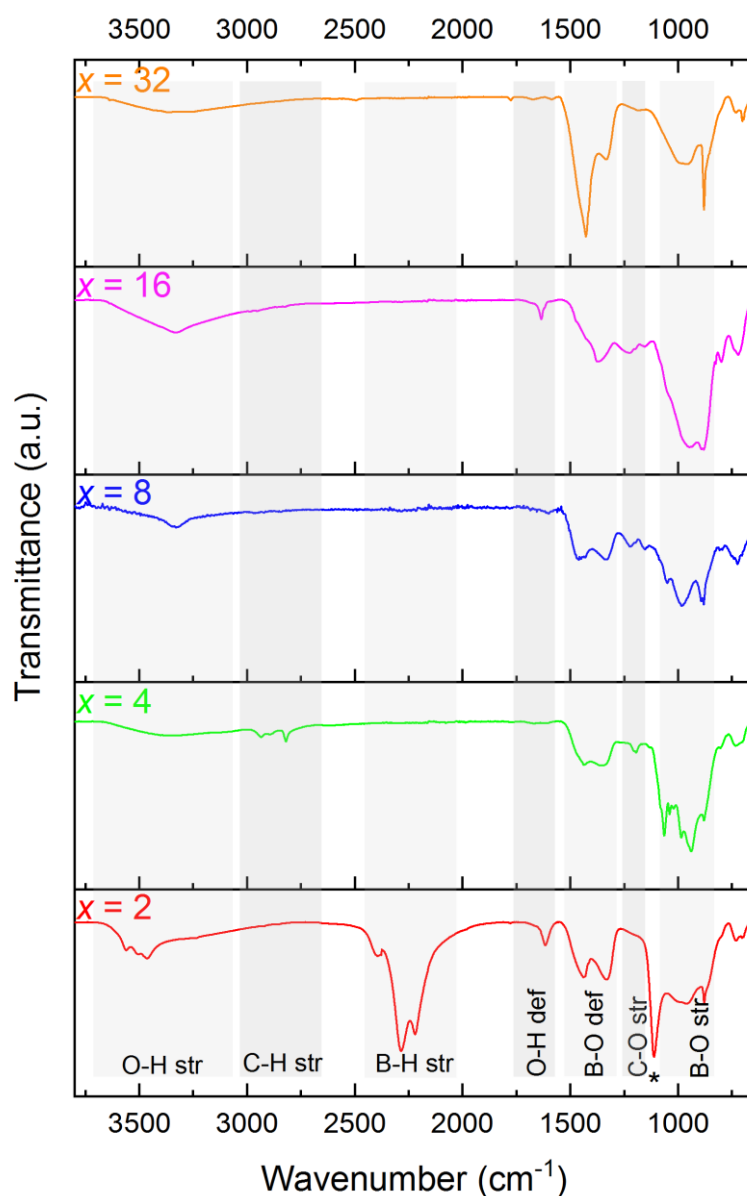
611
 612 **Figure 1.** ^{11}B NMR spectra of the solids recovered after methanolysis of NaBH_4 such as $x = 2, 4, 8, 16$
 613 and 32. The solids were dissolved in N,N-dimethylformamide (with CD_3CN).
 614

615
 616
 617
 618
 619
 620



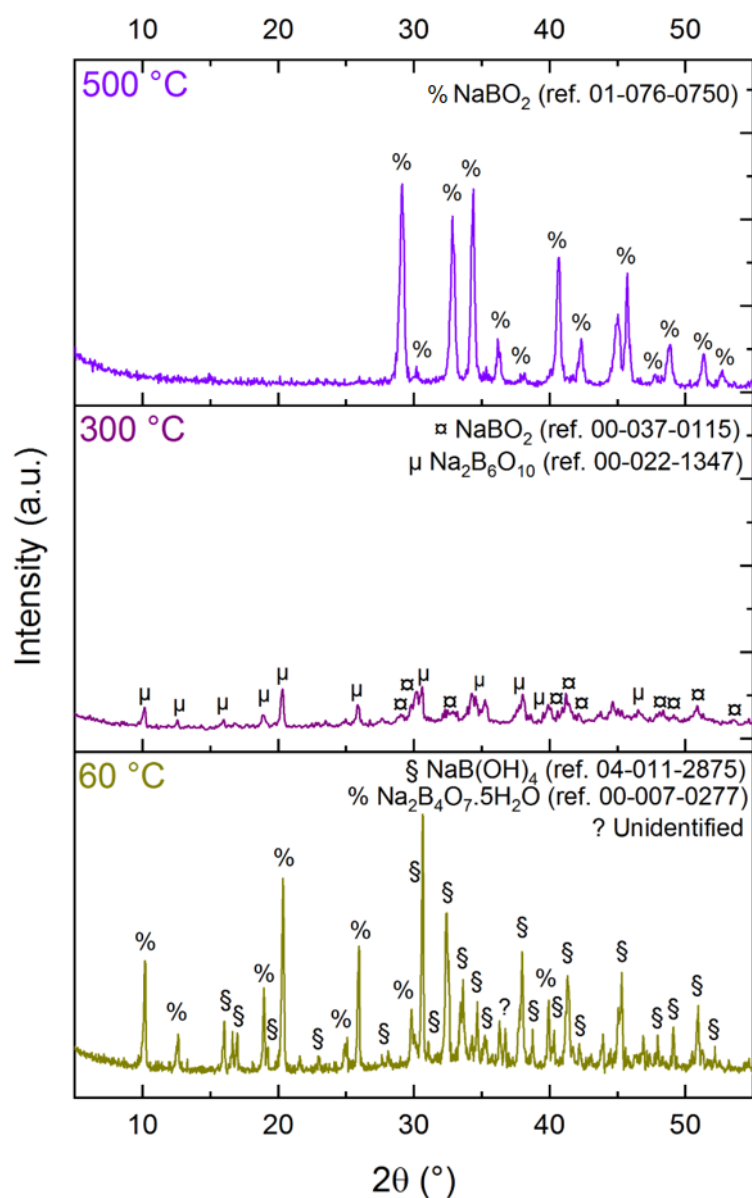
621
 622 **Figure 2.** XRD patterns of the solids recovered after methanolysis of NaBH₄ such as x = 2, 4, 8, 16 and
 623 32. The peaks have been indexed as shown. The structures indicated by # and @ were found to
 624 match with referenced patterns (respectively: NaBH₄ ref. 00-009-0386, and NaB(OCH₃)₄ ref. 00-012-
 625 0863). The structure indicated by & corresponds to that of [Na₂(B(OCH₃)₄)₂(CH₃OH)₂]₄ reported
 626 elsewhere [51]. There are also few unidentified peaks (as shown by the symbol ?).

627
 628
 629
 630
 631



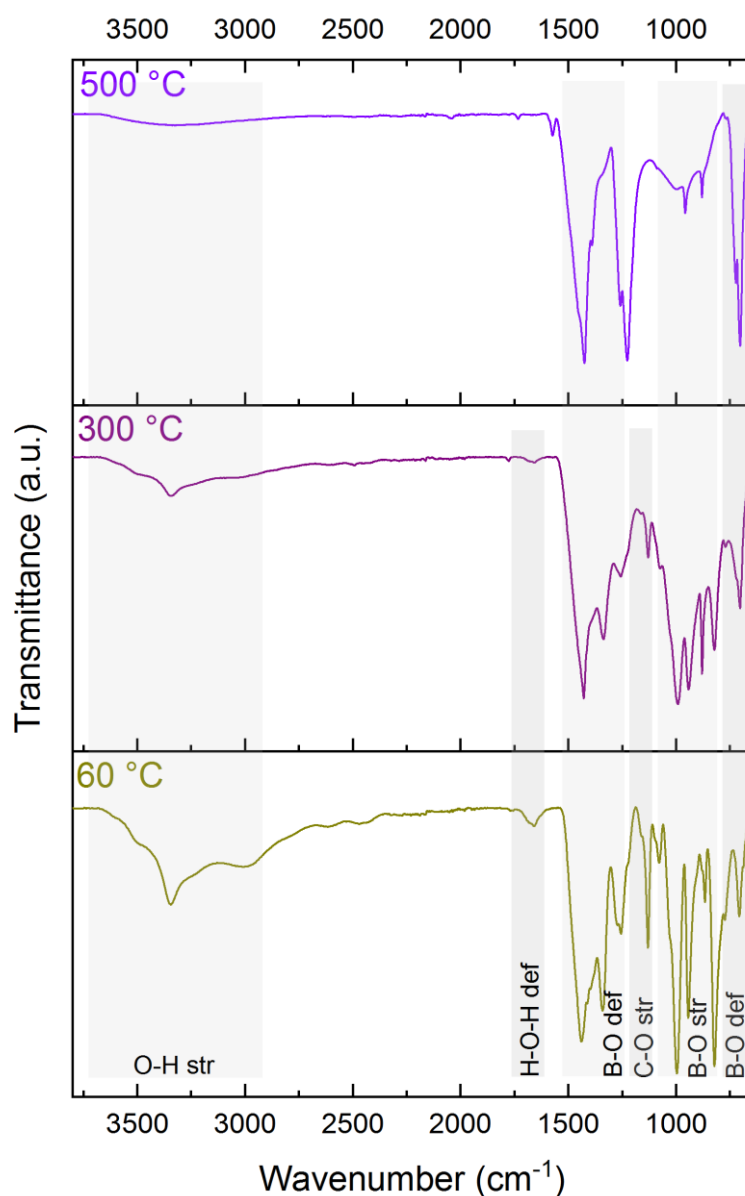
632
 633 **Figure 3.** FTIR spectra of the solids recovered after methanolysis of NaBH₄ such as $x = 2, 4, 8, 16$ and
 634 32. The bands have assigned. The symbol * is attributed to the B–H bending mode. The spectra for x
 635 = 8, 16 and 32 are also shown in Figures S7 to S9.

636
 637
 638
 639
 640
 641

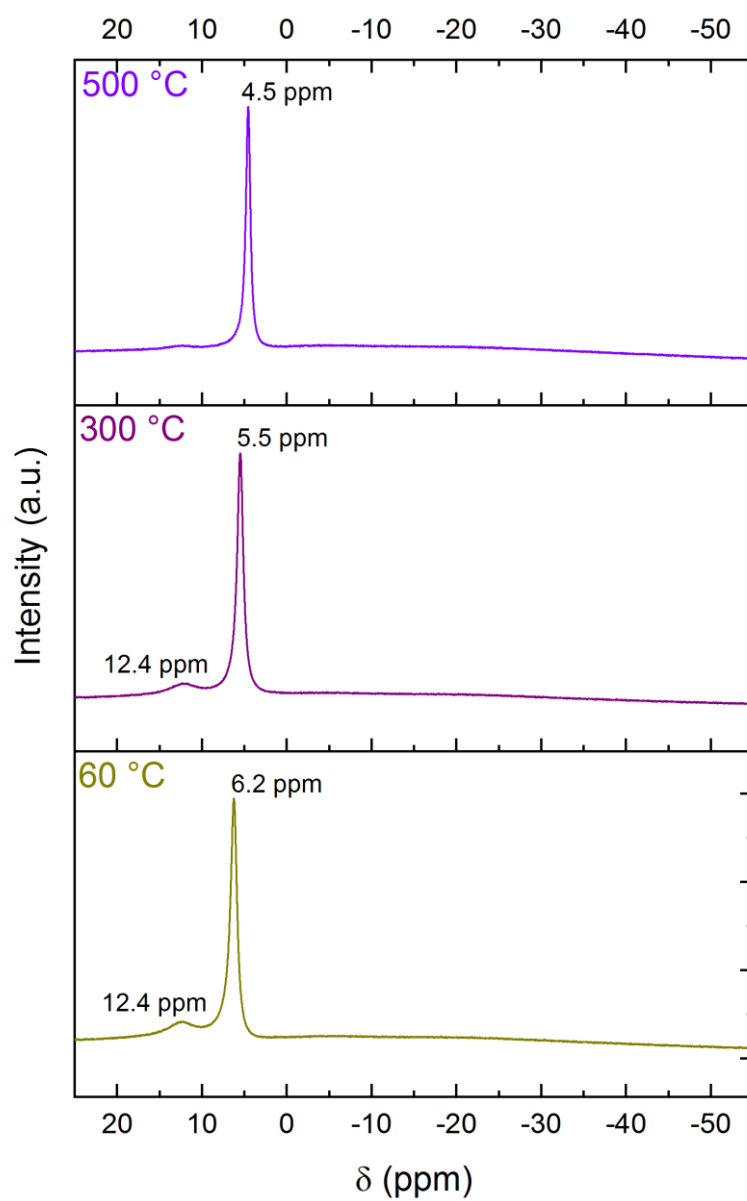


642
 643 **Figure 4.** XRD patterns of the hydrolysis product of $\text{NaB}(\text{OCH}_3)_4$ (i.e. $x = 4$) heated at 60, 300, and 500
 644 °C. The peaks have been assigned, when possible, as shown in the figure. There are few peaks
 645 (shown by the symbol ?) that have not been assigned because of unsuccessful pattern matching.

646
 647
 648
 649
 650
 651

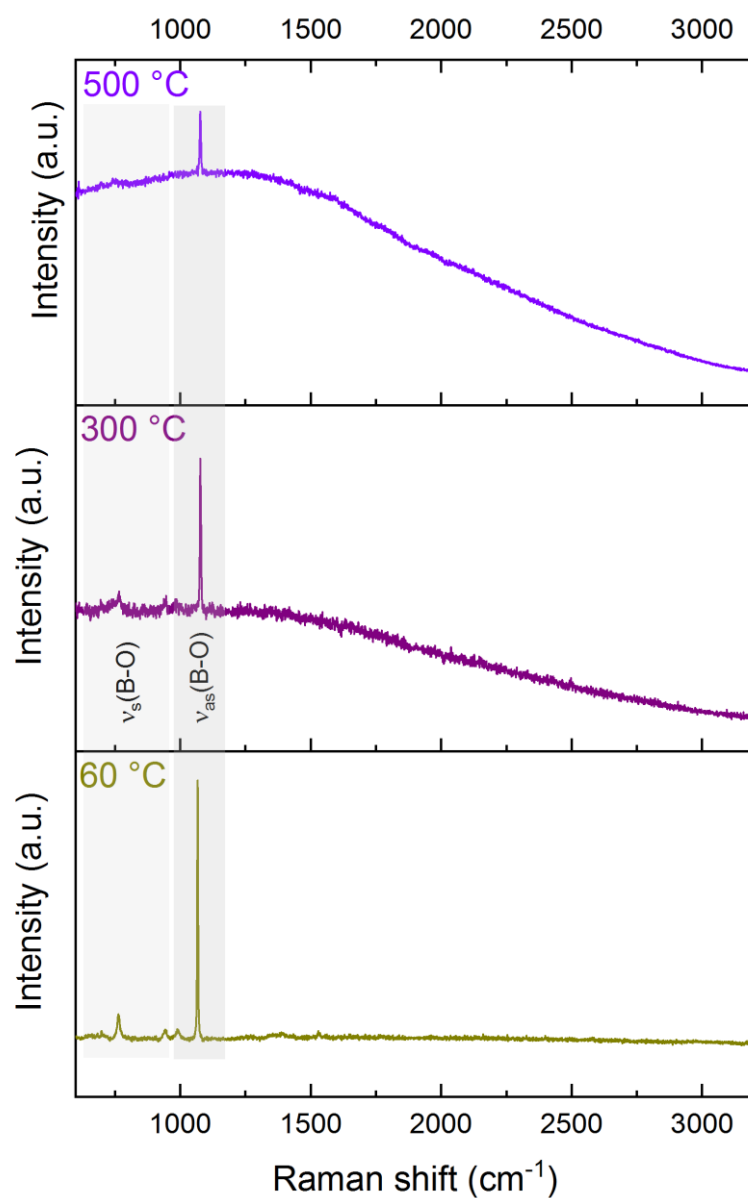


652
 653 **Figure 5.** FTIR spectra of the hydrolysis product of NaB(OCH₃)₄ (i.e. $x = 4$) heated at 60, 300, and 500
 654 °C. The bands have assigned.
 655
 656
 657
 658
 659
 660
 661



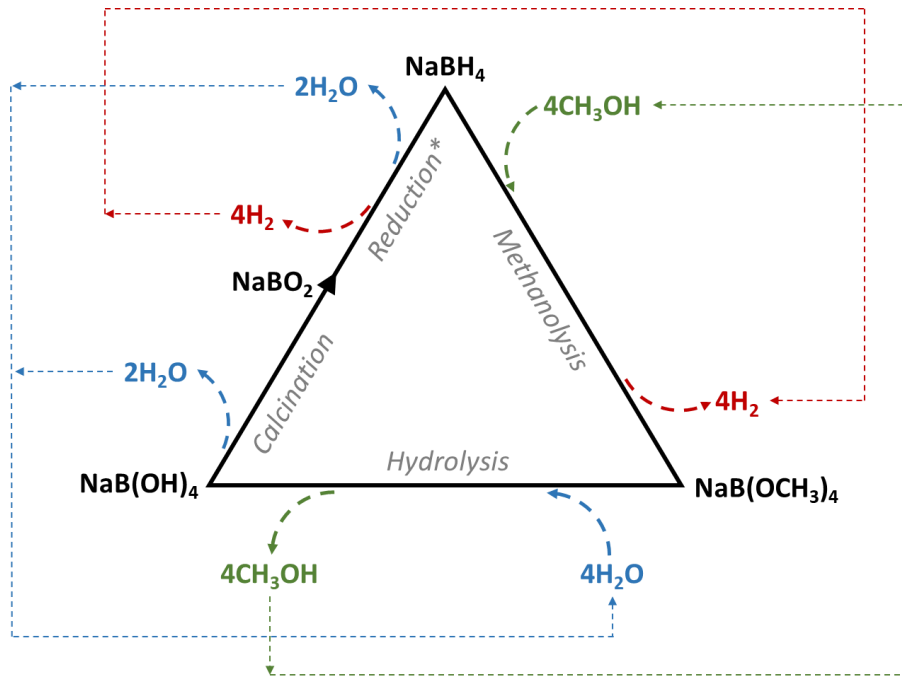
662
663 **Figure 6.** ^{11}B NMR spectra of the hydrolysis product of $\text{NaB}(\text{OCH}_3)_4$ (i.e. $x = 4$) heated at 60, 300, and
664 $500\text{ }^\circ\text{C}$. They were dissolved in deuterated water for analysis.

665
666
667
668
669
670
671



672
 673 **Figure 7.** Raman spectra of the hydrolysis product of $\text{NaB}(\text{OCH}_3)_4$ (i.e. $x = 4$) heated at 60, 300, and
 674 500 °C. The bands have assigned.
 675

676
 677
 678
 679
 680
 681



682
 683
 684
 685
 686
 687
 688
 689
 690
 691
 692
 693
 694
 695
 696
 697
 698
 699
 700
 701
 702

Figure 8. Triangular scheme of the recycling process of the spent fuel stemming from methanolysis of NaBH_4 and subsequent hydrolysis of $\text{NaB}(\text{OCH}_3)_4$. The reduction process transforming NaBO_2 to NaBH_4 requires a reducing agent such H_2 or MgH_2 ; here the scheme has been illustrated with H_2 .

703 **Table 1.** Comparison of the H₂ generation rates (HGR) for a series of hydride-protonic solvent couples
 704 (spontaneous solvolysis reactions without the presence of a catalyst or of an acid).

Hydride	Protonic solvent	T (°C)	HGR (mL H ₂ min ⁻¹)	Ref.
LiBH ₄	H ₂ O	23	2	[64]
NaBH ₄	H ₂ O	20-30	<2	[22,65–67]
NaBH ₄	CH ₃ OH	5	37	[30]
NaBH ₄	CH ₃ OH	20	331	This work
NaBH ₄	CH ₃ OH	45	480	[21]
NaBH ₄	CH ₃ CH ₂ OH	25	<0.1	[68]
KBH ₄	H ₂ O	30	55	[69]
KBH ₄	CH ₃ CH ₂ OH	30	60	[69]
MgH ₂	H ₂ O	25	20	[70]
CaH ₂	H ₂ O	20	3	[71]
NH ₃ BH ₃	H ₂ O	20	<0.1	[64]
NH ₃ BH ₃	CH ₃ OH	20	<0.1	[72]
LiNH ₂ BH ₃	H ₂ O	20	546	[73]
NaNH ₂ BH ₃	H ₂ O	20	381	[74]

705